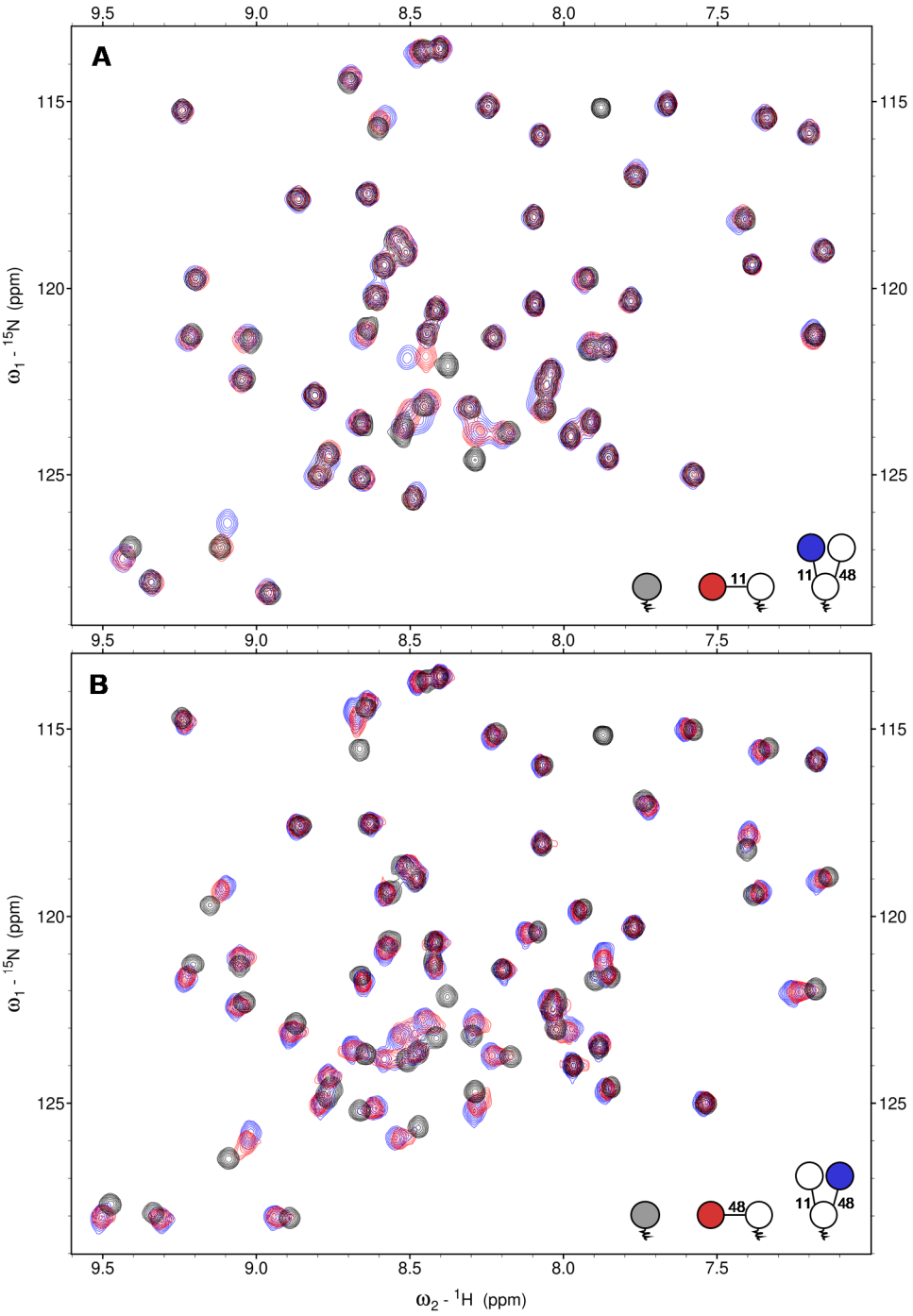

Figure S1: Comparison of NMR spectra of K11-linked and K48-linked Ub. Related to Figure 1. (A) Overlay of ^{1}H-^{15}N SOFAST-HSQC spectra of ^{15}N-monoUb (grey), Ub(^{15}N)–^{11}Ub (red), and Ub(^{15}N)[Ub]–^{11,48}Ub (blue). Signals belonging to select residues are indicated. A color-coded schematic of each (poly)Ub species indicates the ^{15}N-enriched moiety observed in these experiments (bottom right). The corresponding CSPs are shown in Figure 1A. (B) Overlay of ^{1}H-^{15}N SOFAST-HSQC spectra of ^{15}N-monoUb (grey), Ub(^{15}N)–^{48}Ub (red), and Ub[Ub(^{15}N)]–^{11,48}Ub (blue). Signals belonging to select residues are indicated. A color-coded schematic of each (poly)Ub species indicates the ^{15}N-enriched moiety observed in these experiments (bottom right). The corresponding CSPs are shown in Figure 1B.

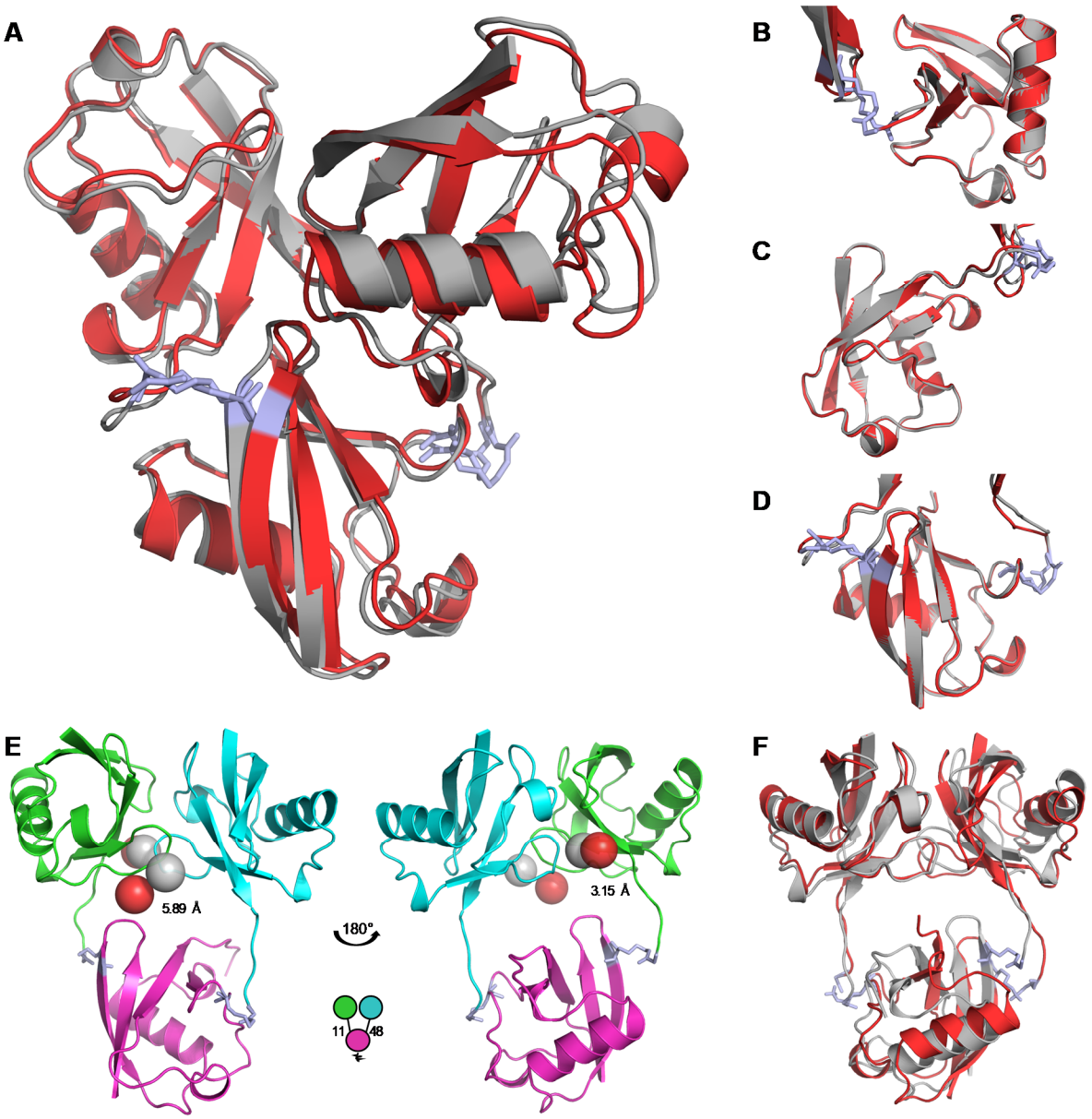

Figure S2: Structures of $[Ub]_2$–^{11,48}Ub. Related to Figures 1 and 2. Two $[Ub]_2$–^{11,48}Ub molecules were present within the asymmetric unit (PDB: 6OQ1). (A) Aligning both structures yields a backbone RMSD of 1.13 Å. However, omitting the flexible tail (residues 72-76) and superimposing only respective monomers improves RMSD values dramatically: (B) 0.23 Å for the distal K11-linked Ub units; (C) 0.30 Å for the distal K48-linked Ub units; and (D) 0.29 Å for the proximal Ub units. This indicates that deviations primarily occur in the flexible linkers, which leads to subtle differences in the orientation and position of each Ub unit, while the tertiary structure of individual Ub units (residues 1-71) are nearly identical. (E) Structure of $[Ub]_2$–^{11,48}Ub generated through TAMC simulation that provides the best match to PRE data (*i.e.* smallest Δ_{MTSL} values). The distal K11-linked Ub is green, the distal K48-linked Ub is cyan, and the proximal Ub is magenta; isopeptide linkages are periwinkle. The distances between the actual (grey spheres) and reconstructed (red spheres) positions of MTSL on the distal K11-linked Ub and distal K48-linked Ub are 5.89 Å and 3.15 Å. (F) The best-match TAMC structure of $[Ub]_2$–^{11,48}Ub (grey) superimposed with the NMR structure (red, PDB: 6OQ2), which yields a backbone RMSD of 4.5 Å.

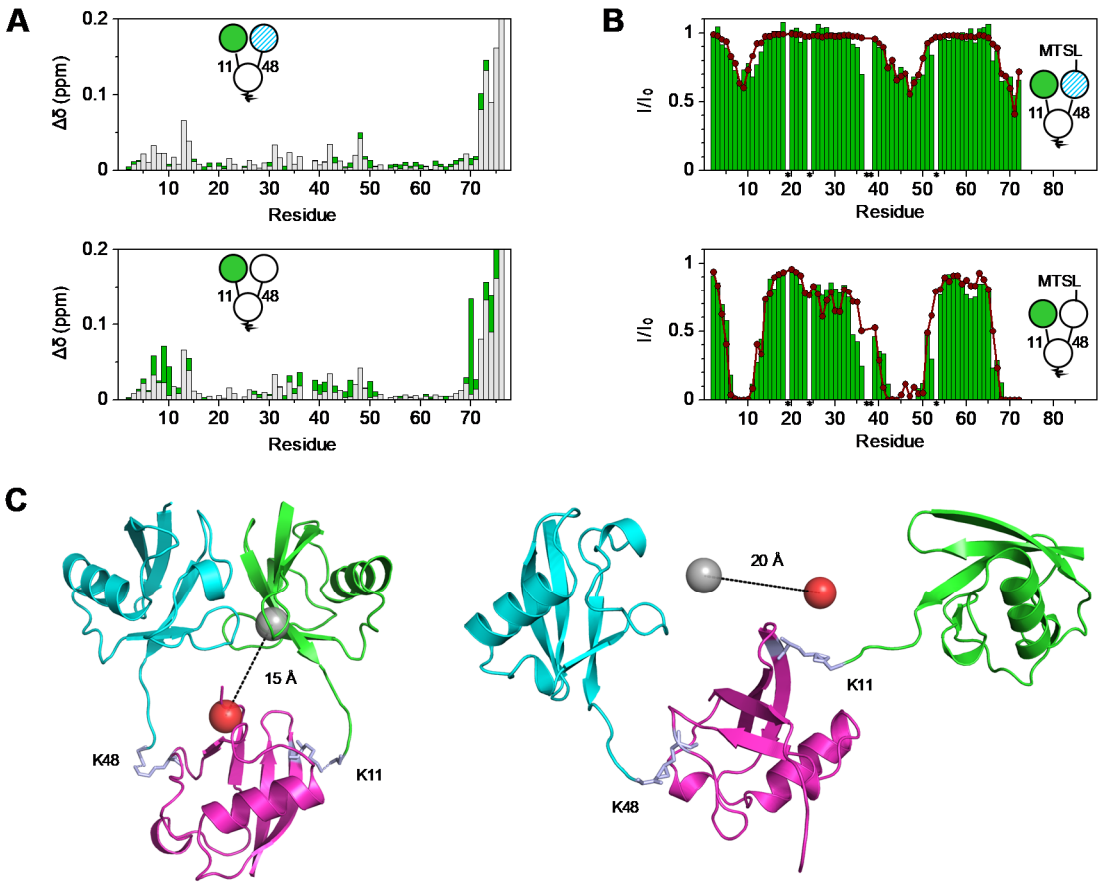

Figure S3: Structural characterization of Ub[Ub$^{L8A/I44A/K48C}$]–^{11,48}Ub. Related to Figures 1 and 2. (A) Overlay of CSPs (Δδ) for Ub(^{15}N)[Ub$^{L8A/I44A/K48C}$]–^{11,48}Ub versus ^{15}N-monoUb (green) and Ub(^{15}N)–^{11}Ub versus ^{15}N-monoUb (light grey). For comparison, the corresponding CSPs for Ub(^{15}N)[Ub]–^{11,48}Ub from Figure 1A are included (bottom). (B) PREs (I/I_0) for Ub(^{15}N)[Ub$^{L8A/I44A/K48C\sim MTSL}$]–^{11,48}Ub. For comparison, the corresponding PREs for Ub(^{15}N)[Ub$^{K48C\sim MTSL}$]–^{11,48}Ub from Figure 2B are included (bottom). Colored bars depict experimental PREs, while red circles represent PREs back-calculated from the reconstructed MTSL position. Residues denoted with an asterisk were not observed in the NMR spectra and not included in analysis. (C) The NMR structure (left, PDB: 6OQ2) and the open conformer (right) of $[Ub]_2$–^{11,48}Ub, where the actual position of the unpaired electron of MTSL attached to C48 of the distal K48-linked Ub is represented by a grey sphere, while the reconstructed MTSL position in Ub[Ub$^{L8A/I44A/K48C\sim MTSL}$]–^{11,48}Ub, the hydrophobic patch mutant, is shown as a red sphere. The distal K11-linked Ub is green, the distal K48-linked Ub is cyan, and the proximal Ub is magenta; isopeptide linkages are periwinkle.

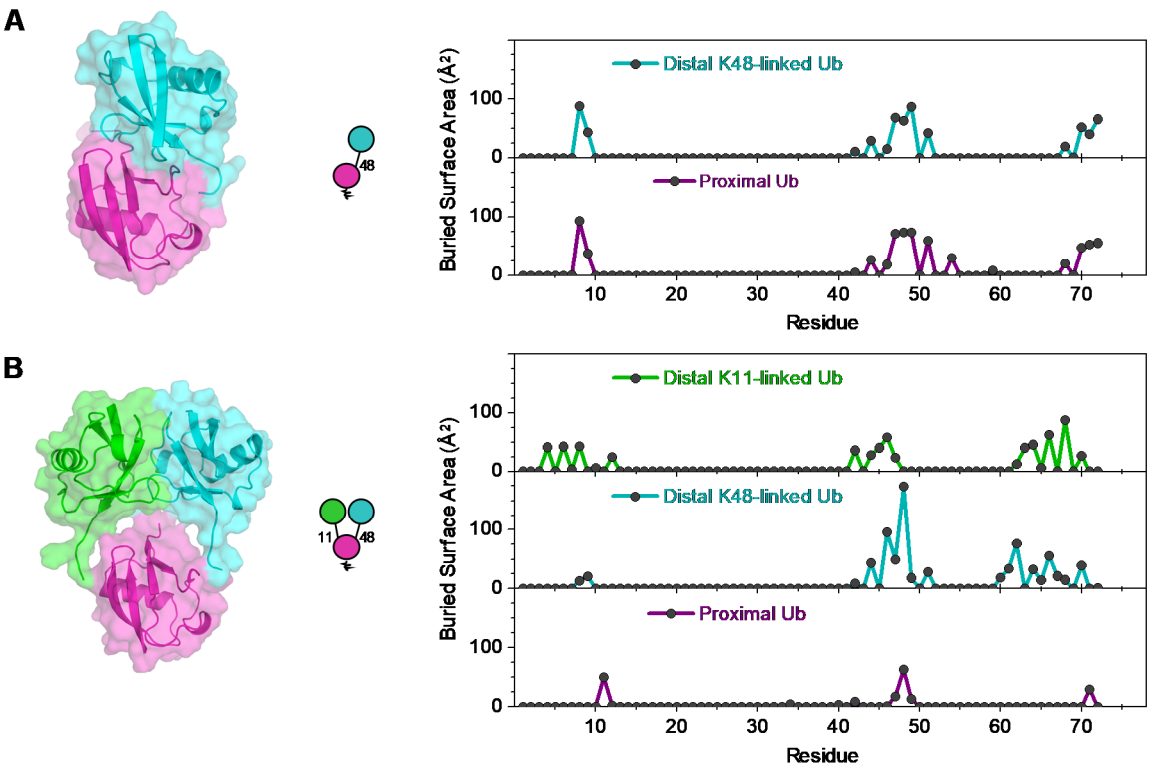

Figure S4: Buried surface area of Ub–^{48}Ub and [Ub]$_2$–^{11,48}Ub. Related to Figure 1. (A) (Left) Surface representation of the Ub–^{48}Ub crystal structure (PDB: 1AAR), which demonstrates the hydrophobic interface between the proximal Ub (magenta) and the distal Ub (cyan). (Right) Buried surface area for each residue of Ub–^{48}Ub; residues with significant buried surface area are components of the interface. The total buried surface area is 1515 Å^2. (B) (Left) Surface representation of the [Ub]$_2$–^{11,48}Ub NMR structure (PDB: 6OQ2), which shows the hydrophobic interface between the distal K11-linked Ub (green) and the distal K48-linked Ub (cyan). (Right) Buried surface area for each residue of [Ub]$_2$–^{11,48}Ub; the distal K11-linked Ub and the K48-linked Ub exhibit buried surface area in and around the hydrophobic patch residues. The only significantly buried residues in the proximal Ub (magenta) of [Ub]$_2$–^{11,48}Ub are K11 and K48, which is a result of being involved in the isopeptide linkages. The total buried surface area is 1539 Å^2. Buried surface areas were determined by GETAREA (Fraczkiewicz and Braun, 1998).

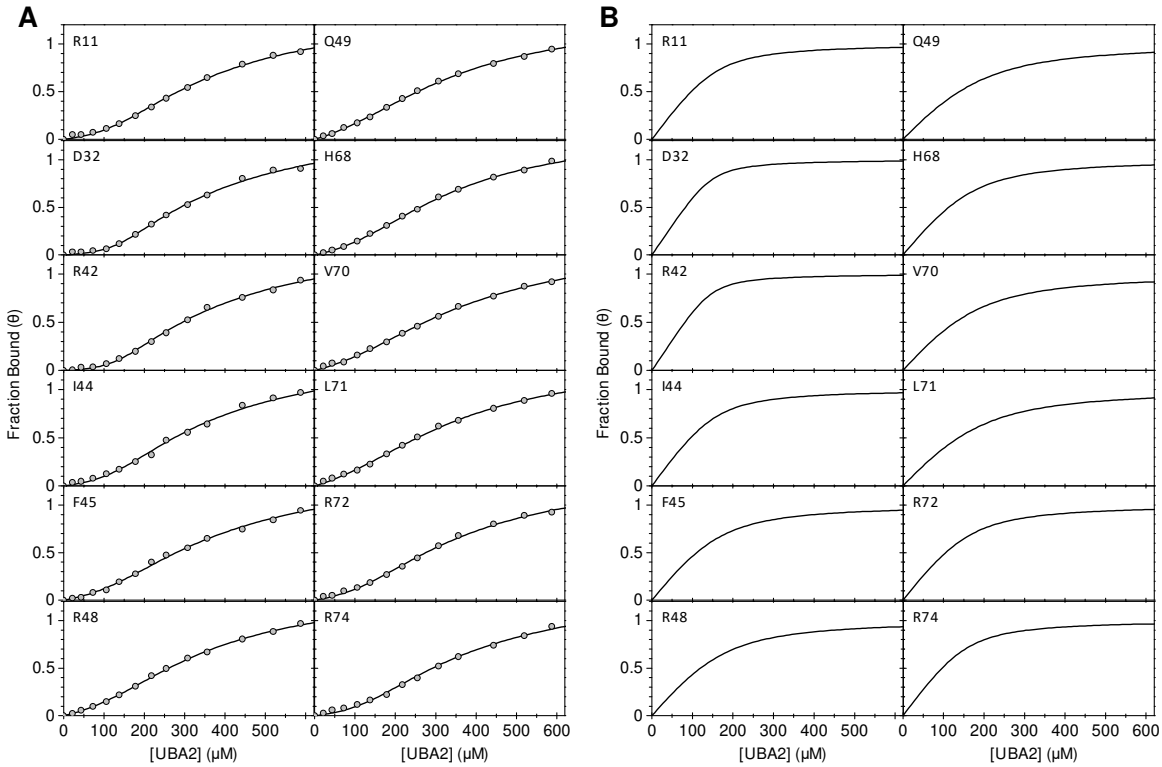

Figure S5: Analysis of UBA2 binding to $[Ub]_2$–^{11,48}Ub using a two-site binding model. Related to Figure 5. CSPs observed in the distal K11-linked Ub were fit to a binding model assuming two independent nonequivalent binding sites/events between Ub(^{15}N)[Ub]–^{11,48}Ub and UBA2. Residues that did not initially shift during the NMR titration but began shifting at an equimolar ratio of UBA2:Ub(^{15}N)[Ub]–^{11,48}Ub were subjected to fitting using the in-house Matlab program Kdfit_2s (Varadan et al., 2004; Varadan et al., 2005b). The calculated bound fraction for each binding site in Ub(^{15}N)[Ub]–^{11,48}Ub (θ) versus total UBA2 concentration is plotted for individual residues. The fits of CSPs observed in the distal K11-linked Ub, reflecting direct binding to the weaker binding site, are shown in (A), and the corresponding back-calculated (although not directly observed) binding events for the tighter UBA2 binding site are shown in (B). The K_d values for the tighter and weaker binding events are 26 ± 13 μM and 248 ± 23 μM, respectively.

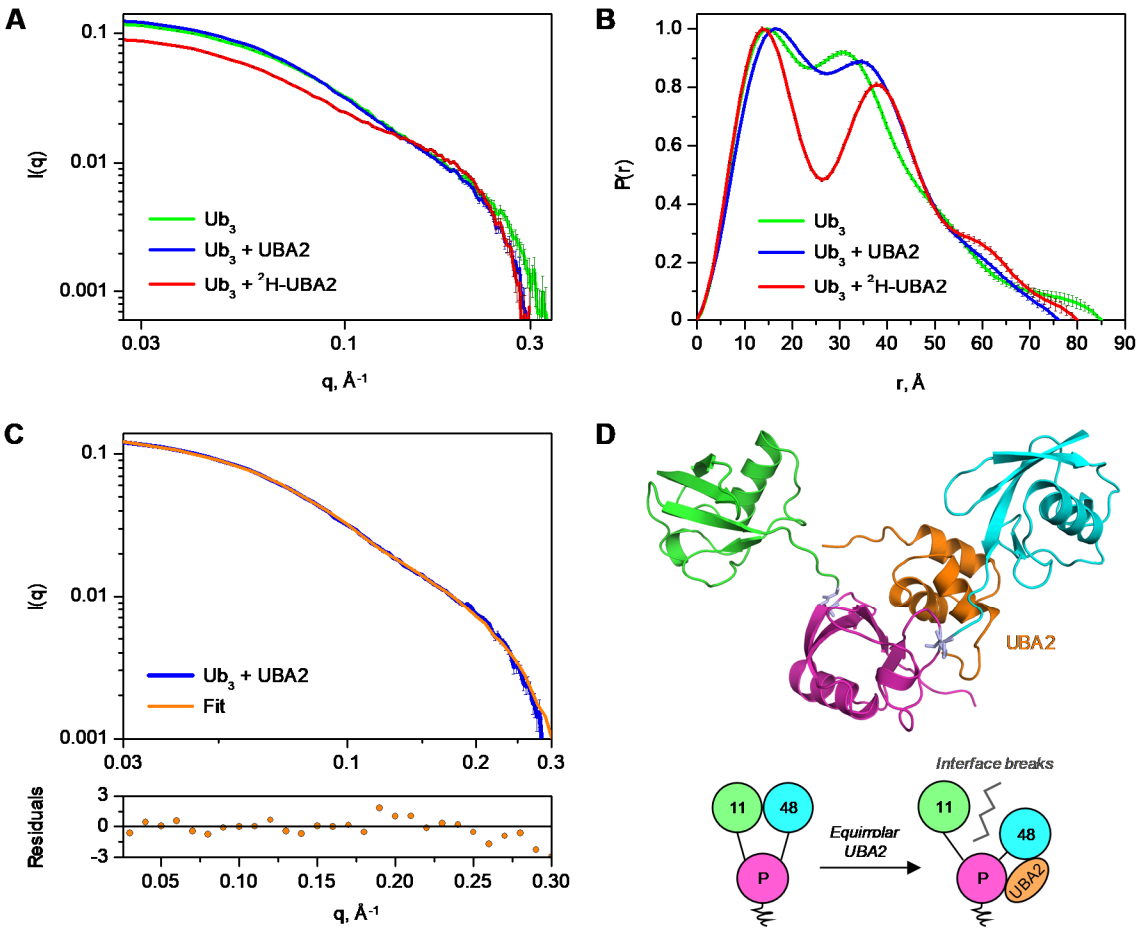

Figure S6: SANS data for $[Ub]_2$–^{11,48}Ub in complex with UBA2. Related to Figures 3 and 5. (A) I(q) and (B) P(r) profiles for $[Ub]_2$–^{11,48}Ub (green), $[Ub]_2$–^{11,48}Ub mixed with an equimolar amount of UBA2 (blue), and $[Ub]_2$–^{11,48}Ub mixed with an equimolar amount of ^{2}H-UBA2 (red). (C) Experimental SANS data, I(q), for $[Ub]_2$–^{11,48}Ub in the presence of equimolar UBA2 (blue) compared to the predicted I(q) (orange line) based on a $[Ub]_2$–^{11,48}Ub:UBA2 complex model, wherein (D) UBA2 intercalates between the distal K48-linked and proximal Ubs, resulting in breakage of the interface between the two distal Ubs. The bottom plot in (C) shows the error-normalized residuals of fit. The distal K11-linked Ub is green, the distal K48-linked Ub is cyan, the proximal Ub is magenta, and UBA2 is orange; isopeptide linkages are periwinkle. The level of ^{2}H-UBA2 deuteration (~82%) provides contrast matching with a 100% D_2O buffer, which renders the ^{2}H-UBA2 component of the complex essentially transparent to neutrons, resulting in a noticeable dip in P(r), seen in (B). Error bars on the SANS data in (A) and (C) are standards errors of the mean based on the number of pixels used in the data averaging. Errors on the P(r) curves in (B) are standard deviations based on multiple fits to the data using a series of Monte Carlo simulations.

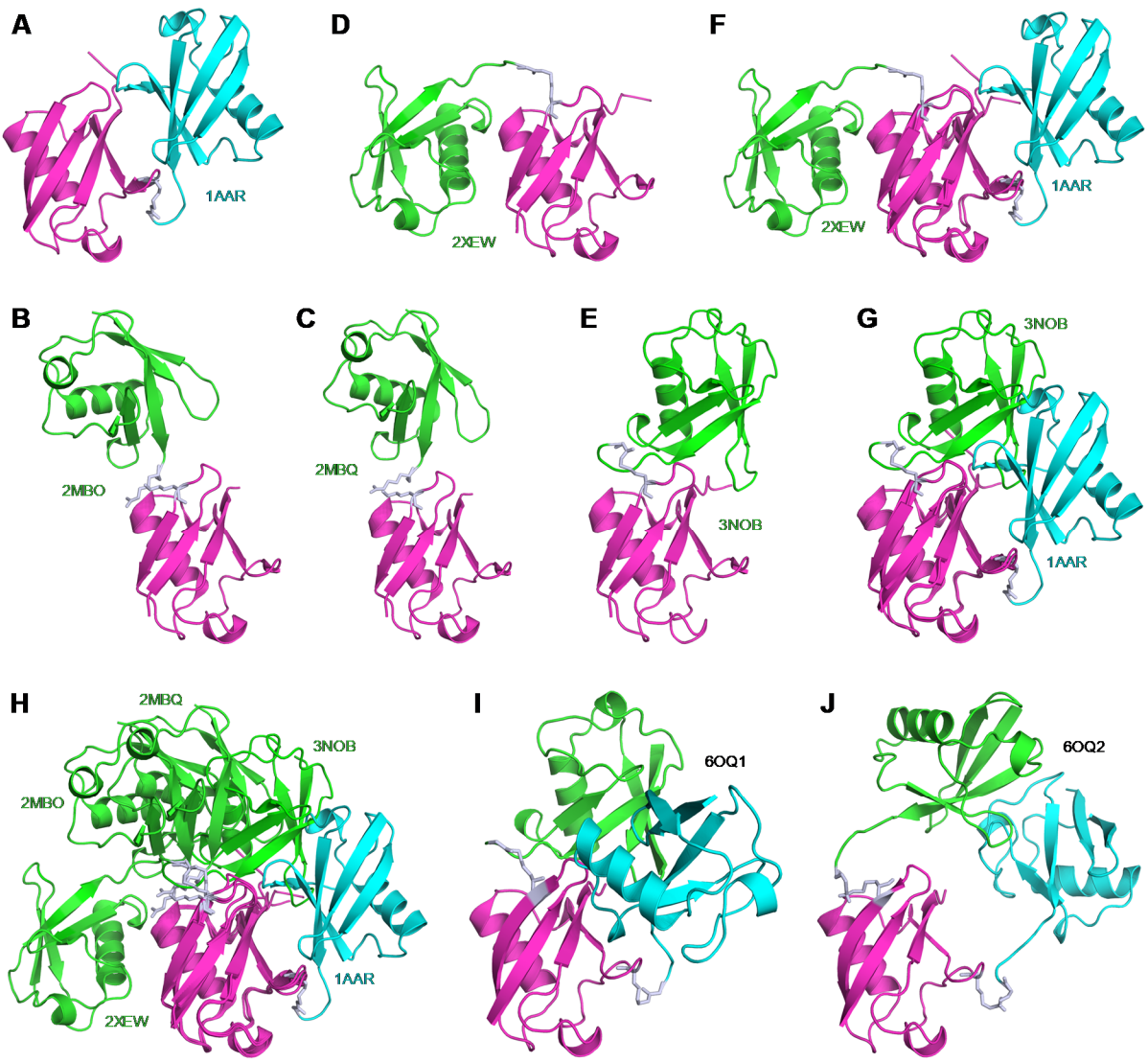

Figure S7: PolyUb structure similarity. Related to Figures 1-3. Comparison of various K11-linked and/or K48-linked polyUb structures, where the distal K11-linked Ub is green, the distal K48-linked Ub is cyan, the proximal Ub is magenta, and isopeptide linkages are periwinkle. (A) Crystal structure of Ub–^{48}Ub (PDB: 1AAR). (B-C) NMR structures of Ub–^{11}Ub (PDB: 2MBO and 2MBQ). (D-E) Crystal structures of Ub–^{11}Ub (PDB: 2XEW and 3NOB). (F) Merged 'open' model of $[Ub]_2$–^{11,48}Ub, with the crystal structures of Ub–^{11}Ub (PDB: 2XEW) and Ub–^{48}Ub (PDB: 1AAR) aligned by the proximal Ub. (G) Merged 'closed' model of $[Ub]_2$–^{11,48}Ub, with the crystal structures of Ub–^{11}Ub (PDB: 3NOB) and Ub–^{48}Ub (PDB: 1AAR) aligned by the proximal Ub. (H) Merged model of $[Ub]_2$–^{11,48}Ub, showing the crystal structures and the NMR structures of Ub–^{11}Ub aligned with the crystal structure of Ub–^{48}Ub (PDB: 1AAR) by the proximal Ub. (I) Crystal structure of $[Ub]_2$–^{11,48}Ub (PDB: 6OQ1). (J) NMR structure of $[Ub]_2$–^{11,48}Ub (PDB: 6OQ2).

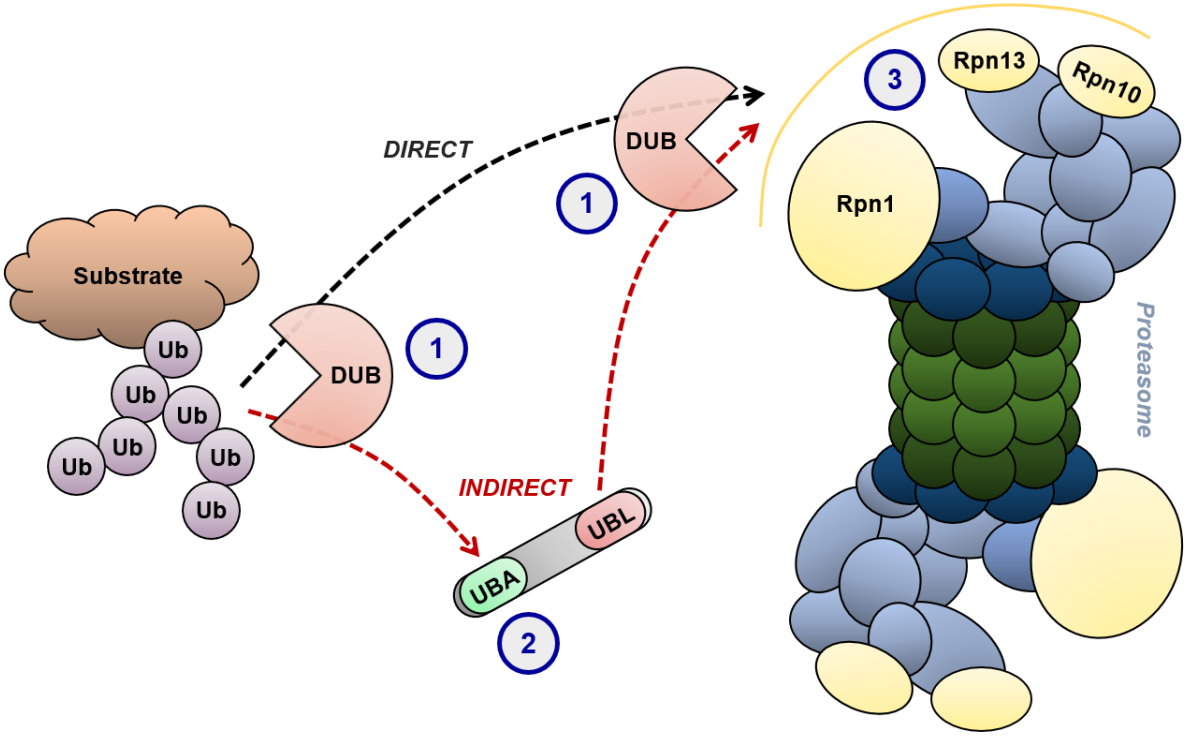

Scheme S1: Ubiquitin-proteasome system (UPS) pathways. Related to Figures 4-6. Schematic of UPS-mediated substrate degradation, highlighting three potential components responsible for enhanced degradation via branched K11/K48-linked polyUb: (1) deubiquitinating (DUB) enzyme activity; (2) proteasomal UBA/UBL shuttle recognition; and (3) proteasomal receptor recognition.

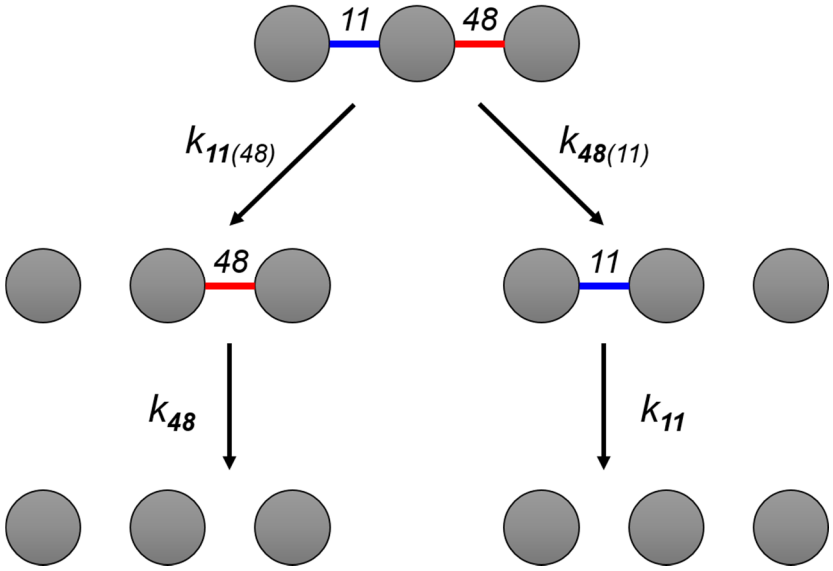

Scheme S2: Disassembly of $[Ub]_2$–^{11,48}Ub by deubiquitinases. Related to Figure 4. Schematic of $[Ub]_2$–^{11,48}Ub disassembly by DUBs into respective products. K11-linkages are shown in blue, while K48-linkages are shown in red. Individual cleavage rate constants are represented by $k_{11(48)}$, $k_{48(11)}$, k_{11}, and k_{48}. The total rate constant for $[Ub]_2$–^{11,48}Ub cleavage into shorter constructs is $k_T = k_{11(48)} + k_{48(11)}$. See Equations 1-4.

Table S1: Nomenclature of the relevant polyubiquitin chains. Related to all Figures.

Ub–^{48}Ub	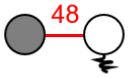 *Distal* Ub(^{15}N)–^{48}Ub	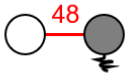 *Proximal* Ub–^{48}Ub(^{15}N)	***Legend:*** *Ub* *^{15}N-labeled Ub* 11 *K11-linkage* 48 *K48-linkage* *Free C-terminus*
Ub–^{48}Ub–^{48}Ub *unbranched*	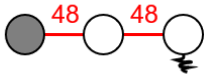 *Distal* Ub(^{15}N)–^{48}Ub–^{48}Ub	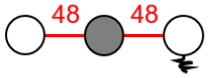 *Middle (Endo)* Ub–^{48}Ub(^{15}N)–^{48}Ub	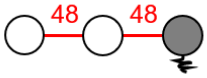 *Proximal* Ub–^{48}Ub–^{48}Ub(^{15}N)
Ub–^{11}Ub–^{48}Ub *unbranched*	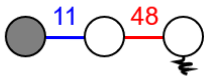 *Distal* Ub(^{15}N)–^{11}Ub–^{48}Ub	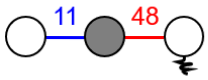 *Middle (Endo)* Ub–^{11}Ub(^{15}N)–^{48}Ub	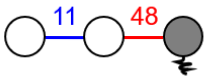 *Proximal* Ub–^{11}Ub–^{48}Ub(^{15}N)
[Ub]$_2$–^{11,48}Ub *branched*	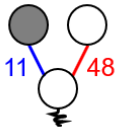 *Distal K11-linked* Ub(^{15}N)[Ub]–^{11,48}Ub	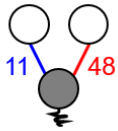 *Proximal* [Ub]$_2$–^{11,48}Ub(^{15}N)	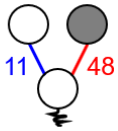 *Distal K48-linked* Ub[Ub(^{15}N)]–^{11,48}Ub

Schematic representation and naming notation (Nakasone et al., 2013) of branched and unbranched polyUb chains used in this study. Ubs are connected by an *en dash* (–); directionality is denoted by arranging the distal Ub(s) on the left and the proximal Ub on the right; residues involved in each linkage are indicated by superscripts; and brackets designate branching from a single Ub. The general name and type of each species is shown in the far-left column. K11-linkages are colored blue and K48-linkages are colored red. ^{15}N-enriched Ub units are shaded gray, as designated by the italicized description in each box; the formal notation is at the bottom of each box. To distinguish between Ub units in the chain, Ub with the free C-terminus is called 'proximal', while the other Ubs (lacking any amino-group linkage) are called 'distal'. Branched mixed-linkage chains contain more than one (distal) Ub attached to the same (proximal) Ub monomer.

Table S2: Deubiquitinase cleavage rate constants. Related to Figure 4.

	OTUB1	Cezanne	IsoT/USP5	USP2	UBP6
$k_{11(48)}$ (hr^{-1})	0.009 ± 0.004	8.3 ± 0.4	8.6 ± 0.2	6.4 ± 0.5	0.04 ± 0.02
$k_{48(11)}$ (hr^{-1})	3.16 ± 0.07	0.33 ± 0.01	2.90 ± 0.05	4.0 ± 0.2	0.31 ± 0.02
k_T (hr^{-1})	3.17 ± 0.07	8.6 ± 0.4	11.5 ± 0.3	10.4 ± 0.6	0.35 ± 0.03
k_{11} (hr^{-1})	0	0.635 ± 0.009	51 ± 1	2.15 ± 0.05	0.149 ± 0.004
k_{48} (hr^{-1})	5.1 ± 0.1	0	11.2 ± 0.2	1.22 ± 0.03	0.367 ± 0.008

The rate constants for cleavage of isopeptide bonds in $[Ub]_2$–^{11,48}Ub. Rates were determined by fitting Equation 4 simultaneously to respective intensities determined from Figure 4, where $k_{11(48)}$, $k_{48(11)}$, k_{11}, and k_{48} correspond to disassembly steps in Scheme S2, while k_T is the sum of $k_{11(48)}$ and $k_{48(11)}$; it represents the combined rate constant of $[Ub]_2$–^{11,48}Ub cleavage into shorter constructs. Boxes with generally similar rate constant values for the same DUB are shaded grey.

Table S3: HADDOCK ambiguous interdomain interaction restraints. Related to Figure 2.

distal K11-linked Ub active residues	7, 8, 9, 10, 11, 14, 36, 39, 40, 46, 48, 71, 72
distal K48-linked Ub active residues	9, 10, 42, 46, 47, 48, 49, 51, 68, 70, 71

Residues with solvent accessibility ≥ 40% and CSPs greater than average for that Ub unit were selected as active residues.

Table S4: HADDOCK unambiguous intermolecular distance restraints. Related to Figure 2.

Isopeptide restraints							
distal K11-linked Ub		**distal K48-linked Ub**		**proximal Ub**		Distance (Å)	Tolerance (Å)
Residue No.	Atom	Residue No.	Atom	Residue No.	Atom		
76	O	-	-	11	N_Z	2.25	0.05
76	C	-	-	11	N_Z	1.35	0.05
76	C	-	-	11	C_E	2.45	0.05
76	C_A	-	-	11	N_Z	2.45	0.05
-	-	76	O	48	N_Z	2.25	0.05
-	-	76	C	48	N_Z	1.35	0.05
-	-	76	C	48	C_E	2.45	0.05
-	-	76	C_A	48	N_Z	2.45	0.05
PRE-derived restraints							
distal K11-linked Ub		**distal K48-linked Ub**		**proximal Ub**		Distance (Å)	Tolerance (Å)
Residue No.	Atom	Residue No.	Atom	Residue No.	Atom		
48	N_E	6	H_N	-	-	17.04	8.0
48	N_E	7	H_N	-	-	17.63	8.0
48	N_E	8	H_N	-	-	17.85	8.0
48	N_E	9	H_N	-	-	17.82	8.0
48	N_E	10	H_N	-	-	15.98	8.0
48	N_E	11	H_N	-	-	18.15	8.0
48	N_E	42	H_N	-	-	19.83	8.0
48	N_E	44	H_N	-	-	16.91	8.0
48	N_E	45	H_N	-	-	16.59	8.0
48	N_E	46	H_N	-	-	14.97	8.0
48	N_E	47	H_N	-	-	13.13	8.0
48	N_E	48	H_N	-	-	15.20	8.0
48	N_E	49	H_N	-	-	17.38	8.0
48	N_E	50	H_N	-	-	19.55	8.0
48	N_E	66	H_N	-	-	18.18	8.0
48	N_E	67	H_N	-	-	18.55	8.0
48	N_E	68	H_N	-	-	16.07	8.0
48	N_E	69	H_N	-	-	16.29	8.0
48	N_E	70	H_N	-	-	16.86	8.0
48	N_E	71	H_N	-	-	15.58	8.0

PRE-derived restraints							
distal K11-linked Ub		**distal K48-linked Ub**		**proximal Ub**		Distance (Å)	Tolerance (Å)
Residue No.	Atom	Residue No.	Atom	Residue No.	Atom		
4	H_N	48	N_E	-	-	17.34	8.0
5	H_N	48	N_E	-	-	15.24	8.0
6	H_N	48	N_E	-	-	11.32	8.0
7	H_N	48	N_E	-	-	10.41	8.0
8	H_N	48	N_E	-	-	6.35	8.0
9	H_N	48	N_E	-	-	8.34	8.0
10	H_N	48	N_E	-	-	9.91	8.0
11	H_N	48	N_E	-	-	12.13	8.0
12	H_N	48	N_E	-	-	15.24	8.0
13	H_N	48	N_E	-	-	14.61	8.0
14	H_N	48	N_E	-	-	18.76	8.0
15	H_N	48	N_E	-	-	19.43	8.0
23	H_N	48	N_E	-	-	19.53	8.0
24	H_N	48	N_E	-	-	19.20	8.0
26	H_N	48	N_E	-	-	19.36	8.0
27	H_N	48	N_E	-	-	17.16	8.0
28	H_N	48	N_E	-	-	18.65	8.0
29	H_N	48	N_E	-	-	19.66	8.0
30	H_N	48	N_E	-	-	17.61	8.0
31	H_N	48	N_E	-	-	17.57	8.0
33	H_N	48	N_E	-	-	19.70	8.0
34	H_N	48	N_E	-	-	18.51	8.0
35	H_N	48	N_E	-	-	18.45	8.0
36	H_N	48	N_E	-	-	16.11	8.0
39	H_N	48	N_E	-	-	16.34	8.0
40	H_N	48	N_E	-	-	14.22	8.0
41	H_N	48	N_E	-	-	12.23	8.0
42	H_N	48	N_E	-	-	8.25	8.0
43	H_N	48	N_E	-	-	10.12	8.0
44	H_N	48	N_E	-	-	8.88	8.0
45	H_N	48	N_E	-	-	11.33	8.0
46	H_N	48	N_E	-	-	12.55	8.0
47	H_N	48	N_E	-	-	11.07	8.0
48	H_N	48	N_E	-	-	12.25	8.0
49	H_N	48	N_E	-	-	11.53	8.0
50	H_N	48	N_E	-	-	11.63	8.0
51	H_N	48	N_E	-	-	15.98	8.0
52	H_N	48	N_E	-	-	17.25	8.0
53	H_N	48	N_E	-	-	19.73	8.0
66	H_N	48	N_E	-	-	16.08	8.0
67	H_N	48	N_E	-	-	13.73	8.0
68	H_N	48	N_E	-	-	9.79	8.0
69	H_N	48	N_E	-	-	8.05	8.0
70	H_N	48	N_E	-	-	6.30	8.0
71	H_N	48	N_E	-	-	5.18	8.0
72	H_N	48	N_E	-	-	8.61	8.0

Restraints were applied to both isopeptide linkages to keep Ub_3 intact during modeling. PRE-derived distance restraints were included for residues with $I/I_0 < 0.8$ in the spin-labeling experiments.